CrossMark

Fabrication and microwave absorption properties of the flaky carbonyl iron/FeSiAl composite in S-band

Peicheng Ji[1] · Guozhi Xie[1] · Ningyan Xie[1] · Jun Li[1] · Jiangwei Chen[1] · Rongqing Xu[1] · Jing Chen[1]

Abstract

The flaky carbonyl iron powder (CIP) was prepared by high-energy ball milling, and then the CIP/FeSiAl composites were obtained with different mass ratios by ultrasonic mixing method in this paper. Here, scanning electron microscopy and Fourier transform infrared spectroscopy were used to demonstrate the microstructure and functional groups of the prepared samples. The element distribution was detected by energy dispersive spectrometer. The complex permittivity and permeability were determined by vector network analysis in the frequency range of 1–18 GHz. The reflection loss (RL) was calculated according to the transmission line theory. The composites exhibit typical flake shapes, which can exceed Snoek limit due to the enhanced shape anisotropy. The results show that the absorption property of composites can be tuned in S-band by changing the mass ratio of CIP and FeSiAl. For the composite (mass ratio of 1:4) with the thickness of only 1 mm, the RL reaches a minimum of -6.4 dB at 2.3 GHz. Moreover, the absorption bandwidth less than -5 dB is 2.3 GHz. This study indicates that the CIP/FeSiAl composites can be potential microwave absorbers in S-band.

1 Introduction

With the rapid development of wireless communications and high-frequency circuit devices, electromagnetic interference (EMI) has grown to a severe problem to be solved [1]. Nowadays the application of absorbing material is one of the most effective means of suppressing EMI [2]. It is well known that the microwave properties of absorbing materials depend heavily on the dielectric and magnetic loss. In order to improve microwave absorption, it is necessary to increase high permeability values, especially high imaginary parts of permeability for absorbing materials [3]. As a traditional soft magnetic material, FeSiAl alloy has been widely employed in absorbing materials due to its high permeability, high saturation flux densities and good machinability [2, 4, 5]. However, the high permittivity (> 50 in general) accompanied with a relatively low permeability in FeSiAl alloy is not conducive to impedance matching [6–8].

For the purpose of obtaining impedance matching, much work has been conducted on FeSiAl to improve its electromagnetic property. Surface modification was regarded as an effective way to decrease the permittivity. Zhang et al. reported they fabricated FeSiAl flakes of good properties after surface modification with nylon [1]. Taghvaei et al. and Fan et al. used organic and inorganic matter respectively as a high resistivity layer to coat on particles' surface [9, 10]. Other researchers found the carbon-based materials had an excellent absorbing property when mixed with magnetic absorbents [11, 12]. As a traditional ultrafine metal powder absorber, the carbonyl iron powder (CIP) possesses a high Curie temperature, the high specific saturation magnetization and the advantage of good temperature stabilization [13]. Compared with FeSiAl, carbonyl iron has a relatively lower permittivity (< 30 in general) and permeability [14]. Increasing electronic devices for special functions in S-band (2–4 GHz) have attracted much attention, such as local area network communication, communication satellites and mobile satellite services [15–17].

In this study, the CIP/FeSiAl composite was fabricated using a simple two-step process. Flaky CIPs were initially prepared by ball milling. Furthermore, we ultrasonically mixed different proportions of prepared CIP and raw FeSiAl alloy to synthesize composite absorbing materials. The microstructure and microwave properties of composites

✉ Guozhi Xie
  guozhixie@njupt.edu.cn

[1] College of Electronic and Optical Engineering & College of Microelectronics, Nanjing University of Posts and Telecommunications, Nanjing 210023, People's Republic of China

were investigated. The aim of this study is to detect the effect of the composite component on the dielectric control mechanism and obtain the excellent S-band absorbing materials.

2 Experimental

The raw materials were commercial FeSiAl alloy and sphere-shaped CIP (purchased from Jiangsu Tianyi Ultrafine metal powder Co., Ltd). The vacuum heat treatment was initially performed on the sphere-shaped CIP at 300 °C for 20 h, which may be conducive to the improvement of electromagnetic properties [18]. Then the annealed powder and ethanol were loaded together with steel balls in a steel container. The milling medium was bearing steel ball with three different diameters (ϕ: 20 mm, ϕ: 8 mm, ϕ: 5 mm). The corresponding ball-to-ball weight ratio was 1:8:8. The ball-to-powder weight ratio was 8:1. The CIP was milled in a planetary ball mill for 8 h at 300 rpm. The as-milled CIP was dried under vacuum at 80 °C for 4 h. The composite was prepared by blending raw FeSiAl with the milled CIP thoroughly in the ultrasonic bath. The mass ratios of CIP and FeSiAl were 4:1, 2:1, 1:1, 1:2 and 1:4, respectively. The mixtures of composite and paraffin were compressed into toroidal-shaped specimens (ϕ_{out}: 7.00 mm, ϕ_{in}: 3.04 mm) with a pressure of 10 MPa for measurements, and the volume fraction of the composite is 75%.

The morphology of the composite was observed by scanning electron microscope (SEM, Hitachi S-3400). The element distribution was detected by energy dispersive spectrometer (EDS, COXEM EM30PLUS). Fourier transform infrared (FTIR) spectra were acquired with a PerkinElmer FTIR (C96926) instrument using KBr wafers. The complex permittivity and permeability (ϵ', ϵ'', μ', μ'') were measured by using Agilent PNA 8363B vector network analyzer with the coaxial-line method in the frequency range of 1–18 GHz. The reflection loss (RL) was calculated according to the transmission line theory [19].

3 Results and discussion

Figure 1a shows the morphology of the raw FeSiAl alloy. The samples exhibit the typical flake shapes, and the average size of the flakes is more than 50 μm. The agglomerate of spherical particle i.e. raw CIP is obviously observed in Fig. 1b. The diameter of the agglomerate is around 50 μm. Figure 1c shows the SEM image of the milled CIP. It can be easily observed that the as-milled powders exhibit a typical microstructure of mechanically milled materials. The as-milled particles are flaky in shape and of rather a broad size distribution. The morphology of composite is also of flaky shape, which is similar to the as-milled CIP, as shown in Fig. 1d. The sizes of the composite are in the range of 5–10 μm. The thicknesses of all particles are below 1 μm, which is beneficial to decrease eddy current loss [20].

Figure 2 shows the elements distribution of 4:1 and 1:4 samples (Back Scattered Electron mode). The existence of

Fig. 1 The SEM image of samples, **a** raw FeSiAl, **b** raw CIP, **c** flaky CIP, **d** CIP/FeSiAl (mass ratio of 1:2) composite
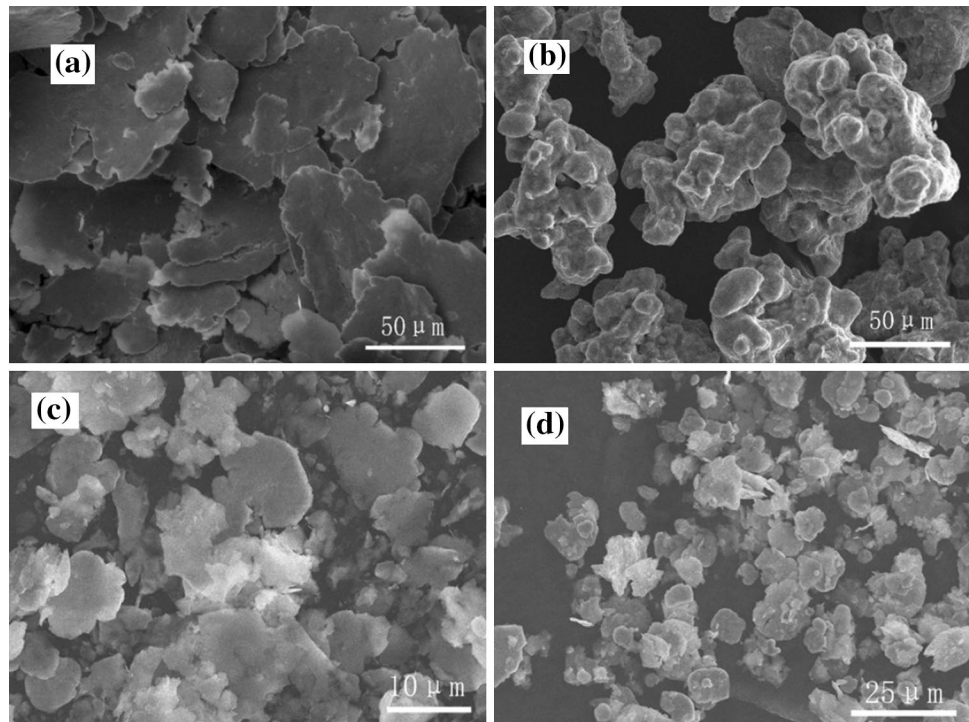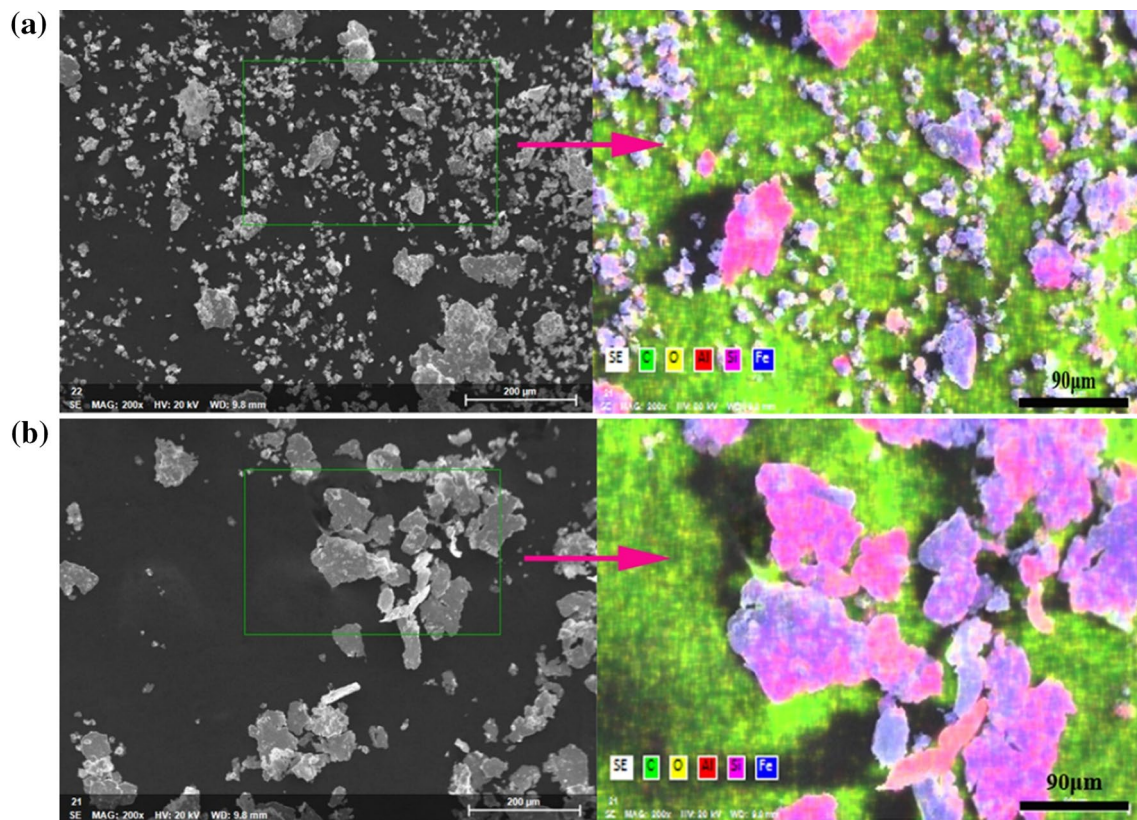
Fig. 2 EDS mappings of composites, **a** CIP/FeSiAl mass ratio of 4:1, **b** CIP/FeSiAl mass ratio of 1:4

element Fe, Si, and Al is confirmed by the EDS mapping. The content of C and O in the composites are very poor. However, it is clearly observed that Fe is distributed uniformly in the composites from Fig. 2a, b. Simultaneously, the element of Fe and Si are the main elements in the composite. There is no doubt that the content of Fe and Si in composites varied with the mass ratio of CIP/FeSiAl.

The FTIR spectrum confirms functional groups in the composites, as shown in Fig. 3. The most significant bands have been identified by comparison with data in Ref [21]. The peak at about 1640 cm^{-1} is assigned to the carbonyl (C=O). It is observed that carbonyl of all samples hardly changes in CIP/FeSiAl composite with different mass ratios, which indicates carbonyl in the composite is not destroyed.

The complex permittivity and permeability spectrum of the raw FeSiAl are shown in Fig. 4a, b. It can be seen that the real part of the complex permittivity is significantly decreased compared to the imaginary permittivity. The ϵ' of raw FeSiAl is relatively higher in S-band. However, the value of ϵ' keeps about 60 after 12 GHz. The imaginary part of permittivity for the raw FeSiAl has little change over the whole 1–18 GHz frequency range. The ϵ'' of raw FeSiAl does not exceed the value of 90. The change of permeability is not obvious comparing to permittivity. The real permeability of raw FeSiAl decreases sharply in S-band, but it is
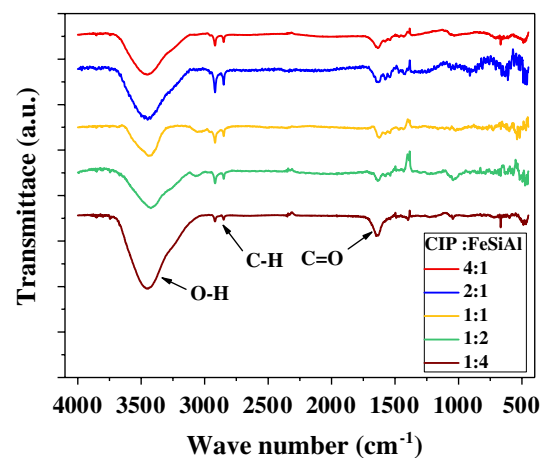
Fig. 3 FTIR spectrum of composites with different CIP/FeSiAl mass ratios

almost constant after 4 GHz. The imaginary part of the complex permeability (μ'') gradually decreases as the frequency increases from 1 to 18 GHz.

Figure 5 shows the complex permittivity of the CIP/FeSiAl composites as a function of the frequency. All samples have their largest ϵ' at 1 GHz. The real permittivity of all samples decreases gradually with increasing
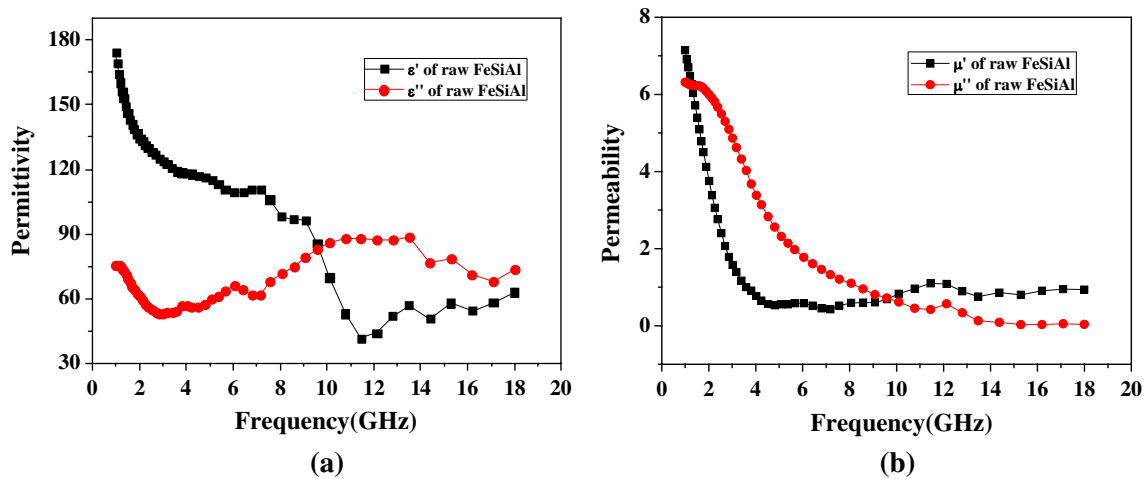
Fig. 4 The permittivity and permeability of raw FeSiAl, **a** the complex permittivity, **b** the complex permeability
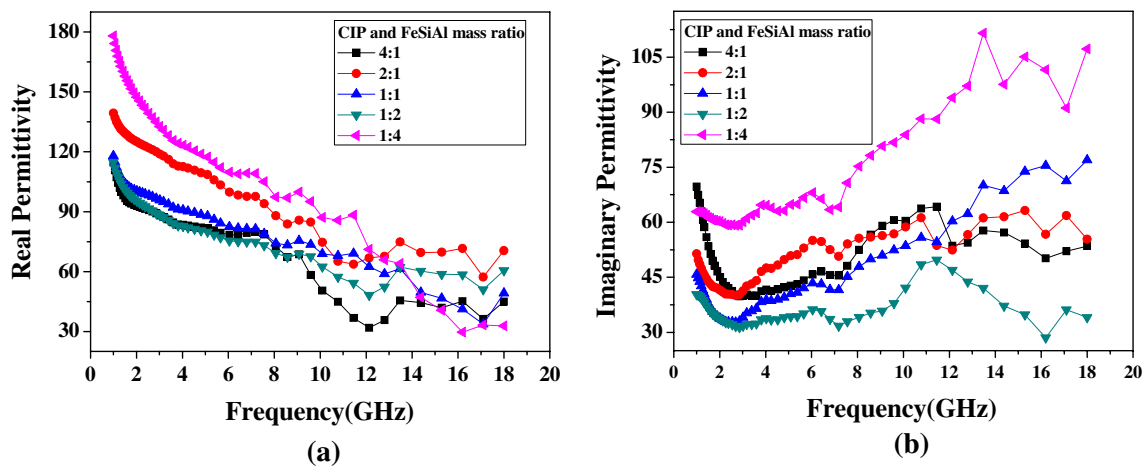

Fig. 5 The permittivity of composites with different CIP and FeSiAl mass ratios, **a** the real permittivity, **b** the imaginary permittivity

the frequency in the 1–18 GHz range, which shows good agreement with the frequency dispersion. The imaginary permittivity of most samples is decreased in low GHz frequency. When the frequency ranges from 4 to 18 GHz, ϵ'' of composites increase with slight oscillates. Feng et al. [22] reported that the dielectric loss is caused by different loss mechanisms as the frequency increases. The increase of permittivity may result from the enhancement of space–charge polarization at the interfaces of particles with the increase of surface area [23, 24]. The role of interface between the CIP/FeSiAl composite should be discussed. It is noted that when the microwave entered into the composite, the polarization arising at the interfaces is due to the migration of charge carriers through different phases of the composite material [25], which results in dielectric relaxation and polarization at the interface. Interfacial polarization always presents in materials comprised of

more than one phase composite [26, 27]. The SEM image also shows a large number of interfaces existed in the CIP/FeSiAl composite. These interfaces play an important role in the composite on the microwave absorption properties and the interface polarization in the composites could facilitate the dielectric loss [7]. The increase in the imaginary permittivity of 1:4 and 1:1 CIP/FeSiAl mass ratios, as the frequency increases, may be the consequence of the increasing interface polarization loss and the electric conductance loss [28]. The composite of 1:4 mass ratio not only has a larger real part of permittivity (ϵ') than others (maximum 180 at 1 GHz) but also a higher imaginary permittivity value. A significant improvement in the dielectric loss as the CIP/FeSiAl mass ratio increased from 1:2 to 1:4 is noted. Thereby, different dielectric losses may be obtained to promote the impedance matching behavior by compounding different proportions of CIP/FeSiAl. These

properties may indicate the component of composites is a major contributor to the dielectric property.

Figure 6 shows the frequency dispersion of the complex permeability for composites. The change of permeability is not obvious comparing to permittivity. Largest μ′ values of all samples are observed at 1 GHz. The μ′ values decrease dramatically in the frequency range 1–4 GHz, which may be due to the domain-wall resonance and relaxation [22]. The real part of the complex permeability (μ′) is decreased with the increasing of FeSiAl content in the 2–6 GHz frequency range, but the difference is very small between 1:1 and 1:2 mass ratio of CIP/FeSiAl. Meanwhile, it can be seen that the μ′ values of the composite are almost the same and present flat curves from 8 to 18 GHz. It is obvious that a significant improvement in the magnetic loss with the addition of FeSiAl in S-band. The imaginary permeability values of all composites exhibit their peaks in S-band and decrease smoothly after 4 GHz. The corresponding peaks of the CIP/FeSiAl composites increase from 5.8 to 10.0 as the CIP/FeSiAl mass ratios change from 4:1 to 1:4. The similar jump of μ″ result was also reported by Yoshida et al. [29]. This characteristic can be attributed to the flake-like particles of the composites. Flake-like particles have lower ferromagnetic resonant frequency and larger permeability than that of spheroids [30]. The high complex permeability of composite is the synergistic effect of the grain refinement, the low eddy current loss and the strong shape anisotropy [14]. Therefore, the complex permeability for the composite absorbing materials is nearly independent of the mass ratio of CIP/FeSiAl in S-band.

Figure 7 shows the typical relationship between RL and frequency for the CIP/FeSiAl composites with the thickness of 1 mm. In general, all samples exhibit excellent S-band absorbing properties. The raw FeSiAl shows a relatively poor performance among all samples with the RL value of
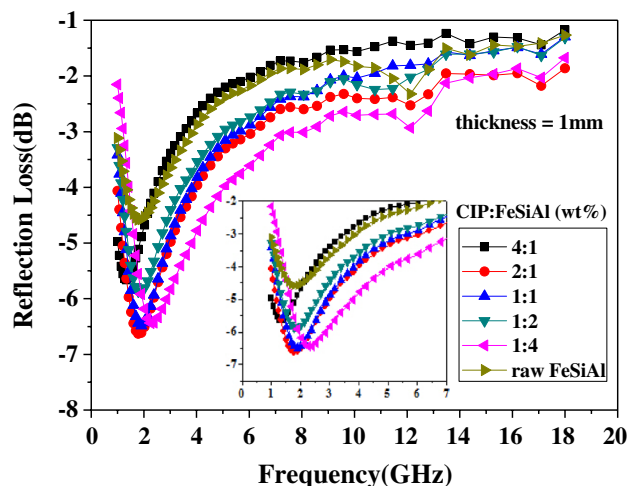

Fig. 7 The RL of the composites with different CIP and FeSiAl mass ratios

−4.5 dB at 1.9 GHz. The results of calculations show that the CIP/FeSiAl composite with the mass ratio of 4:1 also exhibits a relatively poor absorption of only −5.6 dB at 1.4 GHz compared to other composites. The absorption peak of the CIP/FeSiAl (mass ratio of 1:2) composite increases slightly to −5.8 dB at 1.9 GHz. Relative to samples with the mass ratios of 4:1 and 1:2, the samples with mass ratios of 2:1 and 1:1 display stronger microwave absorbing capability with same minimum RL value of −6.5 dB at 2 GHz. The minimum RL of the CIP/FeSiAl composite with mass ratio of 1:4 achieves −6.4 dB at 2.3 GHz. The bandwidth less than −5 dB was 2.3 GHz which was located in the S-band frequencies. The mass ratio of CIP and FeSiAl exerts great influence on the absorbing performance. Though the change of CIP/FeSiAl mass ratio is irregular, it clearly shows that the RL heavily depends on the CIP and FeSiAl mass ratio.
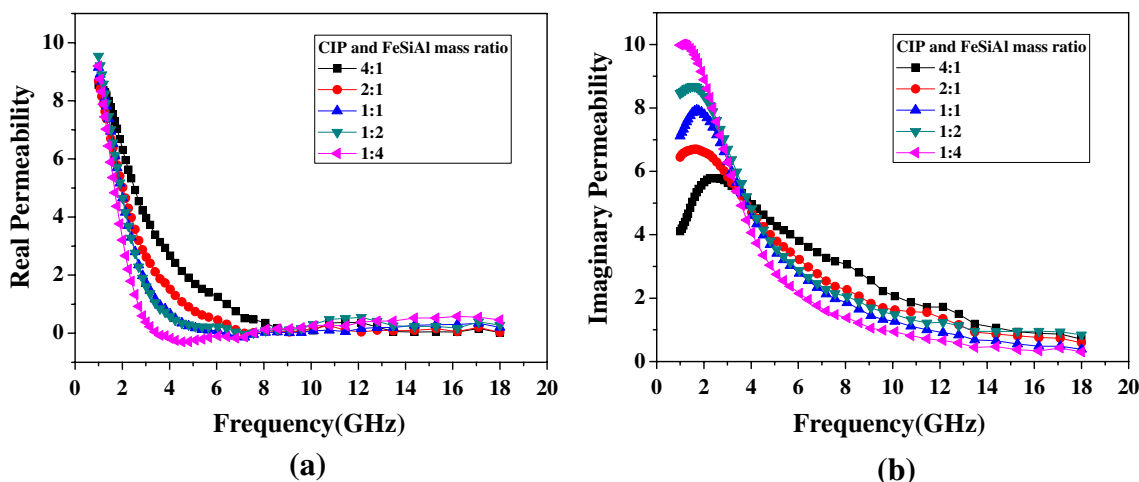

Fig. 6 The permeability of composites with different CIP and FeSiAl mass ratios, **a** the real permeability, **b** the imaginary permeability

The results also indicate that the composites filled with CIP and FeSiAl may have good low frequency absorbing properties as an absorbing material. The lower RL of the composite can be explained by the considerable dielectric loss and magnetic loss in the absorbing materials.

4 Conclusions

The facile synthesis method of CIP/FeSiAl composite was adopted by ultrasonic mixing. The microstructure and the microwave properties of the CIP/FeSiAl composites are investigated in this paper. It is found that carbonyl bond is not destroyed in the CIP/FeSiAl composite over the entire preparation process. The RL_{min} of raw FeSiAl is -4.5 dB at 1.9 GHz. While the CIP and FeSiAl mass ratio is 4:1, the RL peak shift to lowest frequency, and the minimum RL is -5.6 dB at 1.4 GHz, which is beneficial to the application in a lower frequency range. Moreover, the minimum RL of the composite (mass ratio of 1:4) reaches -6.4 dB at 2.3 GHz and the frequency bandwidth ($RL < -5$ dB) is 2.3 GHz. It is found that the microwave properties can be heavily depended on the mass ratio of CIP and FeSiAl, and absorption properties can be tuned in S-band by changing the component of the composite. The flake-shaped CIP/FeSiAl composites exhibit superior electromagnetic properties in S-band due to the comprehensive effects of high dielectric loss property of the FeSiAl and the high planar anisotropy of the flaky CIPs obtained after the ball-milling. The composite with an appropriate mass ratio of CIP and FeSiAl is an attractive candidate for a thin microwave absorbing material in S-band.

References

1. C.K. Zhang, J.J. Jiang, S.W. Bie, L. Zhang, L. Miao, X.X. Xu, J. Alloy. Compd. **527**, 71–75 (2012)
2. W. Zhang, Y. Xu, L. Yuan, J. Cai, D. Zhang, J. Mater. Sci. Technol. **28**, 913–919 (2012)
3. K.N. Rozanov, IEEE Trans. Antennas Propag. **48**, 1230 (2000)
4. T.D. Zhou, P.H. Zhou, D.F. Liang, L.J. Deng, J. Alloy. Compd. **484**, 545–549 (2009)
5. A.H. Kasama, C. Bolfarini, C.S. Kiminami, W.J. Botta Filho, Mater. Sci. Eng. A **449**, 375–377 (2007)
6. K.S. Lee, Y.C. Yun, S.W. Kim, S.S. Kim, J. Appl. Phys. **103**, 07E504 (2008). https://doi.org/10.1063/1.2830827
7. S.S. Kim, S.T. Kim, Y.C. Yoon, K.S. Lee, J. Appl. Phys. **97**, 10F905 (2005). https://doi.org/10.1063/1.1852371
8. A.N. Lagarkov, K.N. Rozanov, J. Magn. Magn. Mater. **321**, 2082–2092 (2009)
9. A.H. Taghvaei, H. Shokrollahi, K.J. Janghorban, J. Alloy. Compd. **481**, 681–686 (2009)
10. X.A. Fan, J. Wang, Z.Y. Wu, G.Q. Li, Mater. Sci. Eng. B **201**, 79–86 (2015)
11. X.F. Zhang, X.L. Dong, H. Huang, B. Lv, J.P. Lei, C.J. Choi, J. Phys. D **40**, 5383–5387 (2007)
12. C. Wang, R. Lv, Z. Huang, F. Kang, J. Gu, J. Alloy. Compd. **509**, 494–498 (2011)
13. J.H. He, W. Wang, J.G. Guan, J. Appl. Phys. **111**, 093924 (2012)
14. L.Y. Zhao, L.D. Zhan, F.C. Zeng et al., Adv. Mater. Res. **1053**, 15–20 (2014)
15. K.W. Kobayashi, A.K. Oki, L.T. Tran, D.C. Streit, IEEE Trans. Microw. Theory Tech. **43**, 3055–3061 (1995)
16. A. Wadhawan, D. Garrett, J.M. Perez, Appl. Phys. Lett. **83**, 2683 (2003)
17. P.C.P. Watts, W.K. Hsu, A. Barnes, B. Chambers, Adv. Mater. **15**(7-8), 600–603 (2003)
18. Y. Qing, W. Zhou, S. Jia, J. Mater. Sci. Technol. **26**(11), 1011–1015 (2010)
19. B. Zhang, Y. Feng, J. Xiong, Y. Yang, H. Lu, IEEE Trans. Magn. **42**, 1778–1781 (2006)
20. J. Sun, H. Xu, Y. Shen et al., J. Alloy. Compd. **548**, 18–22 (2013)
21. R.M. Silverstein, F.X. Webster, *Spectrometric Identification of Organic Compounds*, 6th edn, Chap. 3. (Wiley, New York, 1998).
22. Y.B. Feng, T. Qiu, C.Y. Shen, X.Y. Li, IEEE Trans. Magn. **42**(3), 363–368 (2006)
23. F. Wen, W. Zuo, H. Yi et al., Phys. B **404**, 3567–3570 (2009)
24. H.S. Cho, A.S. Kim, S.M. Kim, J. Namgung, M.C. Kim, G.A. Lee, Phys. Status Solidi A **201**, 1942–1945 (2004)
25. B. Zhao, G. Shao, B. Fan, W. Zhao, R. Zhang, Phys. Chem. Chem. Phys. **17**(8), 6044–6052 (2015)
26. N. Ortega, A. Kumar, R. Katiyar, C. Rinaldi, J. Mater. Sci. **44**, 5127–5142 (2009)
27. S. Wen, Y. Liu, X. Zhao, J. Cheng, H. Li, J. Magn. Magn. Mater. **354**, 7–11 (2014)
28. R.G. Yang, J. Magn. Magn. Mater. **323**, 1805–1810 (2011)
29. S. Yoshida, S. Ando, Y. Shimada et al., J. Appl. Phys. **93**, 6659 (2003)
30. R.M. Walser, W. Win, P.M. Valanju, IEEE Trans. Magn. **34**, 1390 (1998)